arXiv:1209.0156v2 [nucl-ex] 5 Sep 2012

Beyond the Neutron Drip-Line: The Unbound Oxygen Isotopes ^{25}O and ^{26}O

C. Caesar,[1] J. Simonis,[1,2] T. Adachi,[3] Y. Aksyutina,[4,2] J. Alcantara,[5] S. Altstadt,[6] H. Alvarez-Pol,[5] N. Ashwood,[7] T. Aumann,[1,4,*] V. Avdeichikov,[8] M. Barr,[7] S. Beceiro,[5] D. Bemmerer,[9] J. Benlliure,[5] C. A. Bertulani,[10] K. Boretzky,[4] M.J.G. Borge,[11] G. Burgunder,[12] M. Caamano,[5] E. Casarejos,[5] W. Catford,[13] J. Cederkäll,[8] S. Chakraborty,[14] M. Chartier,[15] L. Chulkov,[16,2] D. Cortina-Gil,[5] U. Datta Pramanik,[14] P. Diaz Fernandez,[5] I. Dillmann,[4] Z. Elekes,[9] J. Enders,[1] O. Ershova,[6] A. Estrade,[4] F. Farinon,[4] L. M. Fraile,[17] M. Freer,[7] M. Freudenberger,[1] H.O.U. Fynbo,[18] D. Galaviz,[19] H. Geissel,[4] R. Gernhäuser,[20] P. Golubev,[8] D. Gonzalez Diaz,[1] J. Hagdahl,[21] T. Heftrich,[6] M. Heil,[4] M. Heine,[1] A. Heinz,[21] A. Henriques,[19] M. Holl,[1] J. D. Holt,[22,23] G. Ickert,[4] A. Ignatov,[1] B. Jakobsson,[8] H.T. Johansson,[21] B. Jonson,[21] N. Kalantar,[3] R. Kanungo,[24] A. Kelic-Heil,[4] R. Knöbel,[4] T. Kröll,[1] R. Krücken,[20,†] J. Kurcewicz,[4] M. Labiche,[25] C. Langer,[6] T. Le Bleis,[20] R. Lemmon,[25] O. Lepyoshkina,[20] J. Machado,[19] J. Marganiec,[2] V. Maroussov,[26] J. Menéndez,[1,2] M. Mostazo,[5] A. Movsesyan,[1] A. Najafi,[3] T. Nilsson,[21] C. Nociforo,[4] V. Panin,[1] A. Perea,[11] S. Pietri,[4] R. Plag,[6] A. Prochazka,[4] A. Rahaman,[14] G. Rastrepina,[4] R. Reifarth,[6] G. Ribeiro,[11] M.V. Ricciardi,[4] C. Rigollet,[3] K. Riisager,[18] M. Röder,[27,9] D. Rossi,[4] J. Sanchez del Rio,[11] D. Savran,[2,28] H. Scheit,[1] A. Schwenk,[2,1] H. Simon,[4] O. Sorlin,[12] V. Stoica,[3] B. Streicher,[3] J. Taylor,[15] O. Tengblad,[11] S. Terashima,[4] R. Thies,[21] Y. Togano,[2] E. Uberseder,[29] J. Van de Walle,[3] P. Velho,[19] V. Volkov,[1] A. Wagner,[9] F. Wamers,[1] H. Weick,[4] M. Weigand,[6] C. Wheldon,[7] G. Wilson,[13] C. Wimmer,[6] J. Winfield,[4] P. Woods,[30] D. Yakorev,[9] M.V. Zhukov,[21] A. Zilges,[26] M. Zoric,[4] and K. Zuber[27]
(R3B collaboration)

[1] *Institut für Kernphysik, Technische Universität Darmstadt, 64289 Darmstadt, Germany*
[2] *ExtreMe Matter Institute EMMI, GSI Helmholtzzentrum für Schwerionenforschung GmbH, 64291 Darmstadt, Germany*
[3] *KVI, University of Groningen, Zernikelaan 25, NL-9747 AA Groningen, The Netherlands*
[4] *GSI Helmholtzzentrum für Schwerionenforschung, D-64291 Darmstadt, Germany*
[5] *Departamento de Física de Partículas, Universidade de Santiago de Compostela, 15706 Santiago de Compostela, Spain*
[6] *Goethe-Universität Frankfurt am Main, 60438 Frankfurt am Main, Germany*
[7] *School of Physics and Astronomy, University of Birmingham, Birmingham B15 2TT, United Kingdom*
[8] *Department of Physics, Lund University, S-22100 Lund, Sweden*
[9] *Helmholtz-Zentrum Dresden-Rossendorf, D-01328 Dresden, Germany*
[10] *Department of Physics and Astronomy, Texas A&M University-Commerce, Commerce, Texas 75429, USA*
[11] *Instituto de Estructura de la Materia, CSIC, Serrano 113 bis, E-28006 Madrid, Spain*
[12] *Grand Accélérateur National d'Ions Lourds (GANIL),*
CEA/DSM-CNRS/IN2P3, B.P. 55027, F-14076 Caen Cedex 5, France
[13] *Department of Physics, University of Surrey, Guildford GU2 5XH, United Kingdom*
[14] *Saha Institute of Nuclear Physics, 1/AF Bidhan Nagar, Kolkata-700064, India*
[15] *Oliver Lodge Laboratory, University of Liverpool, Liverpool L69 7ZE, United Kingdom*
[16] *Kurchatov Institute, Ru-123182 Moscow, Russia*
[17] *Facultad de Ciencias Fsicas, Universidad Complutense de Madrid, Avda. Complutense, E-28040 Madrid, Spain*
[18] *Department of Physics and Astronomy, Aarhus University, DK-8000 Århus C, Denmark*
[19] *Centro de Fisica Nuclear, University of Lisbon, P-1649-003 Lisbon, Portugal*
[20] *Physik Department E12, Technische Universität München, 85748 Garching, Germany*
[21] *Fundamental Fysik, Chalmers Tekniska Högskola, S-412 96 Göteborg, Sweden*
[22] *Department of Physics and Astronomy, University of Tennessee, Knoxville, TN 37996, USA*
[23] *Physics Division, Oak Ridge National Laboratory, P.O. Box 2008, Oak Ridge, TN 37831, USA*
[24] *Astronomy and Physics Department, Saint Mary's University, Halifax, NS B3H 3C3, Canada*
[25] *STFC Daresbury Laboratory, Daresbury, Warrington WA4 4AD, United Kingdom*
[26] *Institut für Kernphysik, Universität zu Köln, D-50937 Köln, Germany*
[27] *Institut für Kern- und Teilchenphysik, Technische Universität, 01069 Dresden, Germany*
[28] *Frankfurt Institut for Advanced Studies FIAS, Frankfurt, Germany*
[29] *Department of Physics, University of Notre Dame, Notre Dame, Indiana 46556, USA*
[30] *School of Physics and Astronomy, University of Edinburgh, Edinburgh EH9 3JZ, United Kingdom*

(Dated: 31-August-2012)

The very neutron-rich oxygen isotopes ^{25}O and ^{26}O are investigated experimentally and theoretically. In this first R3B-LAND experiment, the unbound states are populated at GSI via proton-knockout reactions from ^{26}F and ^{27}F at relativistic energies around 450 MeV/nucleon. From the kinematically complete measurement of the decay into ^{24}O plus one or two neutrons, the ^{25}O ground-state energy and lifetime are determined, and upper limits for the ^{26}O ground state are extracted. In addition, the results provide evidence for an excited state in ^{26}O at around 4 MeV. The experimental findings are compared to theoretical shell-model calculations based on chiral two- and three-nucleon (3N) forces, including for the first time residual 3N forces, which are shown to be amplified as valence neutrons are added.

PACS numbers: 21.10.-k, 25.60.t, 27.30.+t, 29.30.Hs

Understanding the properties of nuclei with extreme neutron-to-proton ratios presents a major challenge for rare-isotope beam experiments and nuclear theory. Nuclei located at and beyond the neutron dripline play a crucial role in this endeavor. Experimentally, the neutron dripline has been established up to oxygen [1] with ^{24}O being the last bound isotope, while it extends considerably further in fluorine [2], providing first experimental evidence for the particle stability of ^{31}F and particle instability of ^{28}O. Recently, it has been shown that the anomalous behavior in the oxygen isotopes is due to the impact of 3N forces, which provide repulsive contributions to the interactions of valence neutrons [3], connecting the frontier of neutron-rich nuclei to the theoretical developments of nuclear forces.

Another striking feature in oxygen is the doubly magic nature of ^{22}O and ^{24}O [1, 4–6] in strong contrast to the lighter elements, where the dripline is marked by nuclei exhibiting a loosely-bound halo structure. The neutron-rich oxygen isotopes also provide interesting insights, when viewed coming from stable nuclei. As protons are removed along isotones, the attractive contribution from the proton-neutron tensor force decreases, thus, opening up the $N = 16$ neutron shell for oxygen [7], which is below the $N = 20$ magic number present in stable nuclei.

How the structure proceeds beyond ^{24}O towards $N = 20$ is thus of central interest. The present experimental limits are ^{25,26}O, for which a resonance energy and width have been reported for ^{25}O [4] and a resonance position for ^{26}O [8]. Those experiments had a limited acceptance for neutrons, resulting in a narrow energy window to which the experiment was sensitive [9]. In this first R3B-LAND experiment, we investigate both unbound isotopes ^{25,26}O with an essentially flat efficiency up to 8 MeV relative energy. It has been speculated that the unbound isotopes ^{26}O and ^{28}O might have a rather long lifetime, which would constitute the first example of neutron radioactivity [10]. Our present result establishes a firm upper limit for the lifetime of the ^{26}O ground state. We then combine the experimental investigation with theoretical calculations based on chiral two-nucleon (NN) and 3N forces, where we focus on the increasing contribution from residual three-neutron forces as neutrons are added.

The experiment has been carried out at the GSI Helmholtzzentrum in Darmstadt using the R3B-LAND reaction setup. Beams of light neutron-rich nuclei have been produced by fragmentation reactions of a 490 MeV/nucleon ^{40}Ar primary beam in a 4 g/cm^2 Be target. Ions with a magnetic rigidity of 9.88(±1%) Tm corresponding to an A/Z ratio of around 3 have been selected by the fragment separator FRS and transported to the experimental area. Energy-loss and time-of-flight measurements served for identification of the incoming ions on an event-by-event basis. The beam cocktail contained ^{26,27}F ions, which were selected to populate the unbound states in ^{25,26}O, by one-proton knockout reactions. Different targets have been used, while most of the statistics stems from measurements with the CH$_2$ (922 mg/cm^2) target. The target was surrounded by the 4π detector Crystal Ball consisting of 160 NaI crystals for detecting photons and light particles emitted at large angles. Position and energy loss of the beam and fragments behind the target were detected by two silicon strip detectors before deflection in the large-gap dipole magnet ALADIN. Two further position measurements after the magnet with scintillating fiber detectors served for tracking of the ions through the dipole field. Together with time-of-flight and energy-loss measurements, this yields the magnetic rigidity and atomic number and thus the mass of the fragments. Neutrons from the decay of unbound states were detected at a distance of around 12 m downstream the target by the LAND neutron detector with an efficiency of 92% for one neutron events and covering an angular range of ±80 mrad around the beam axis. A similar experimental setup and analysis scheme is described in Ref. [11] in more detail.

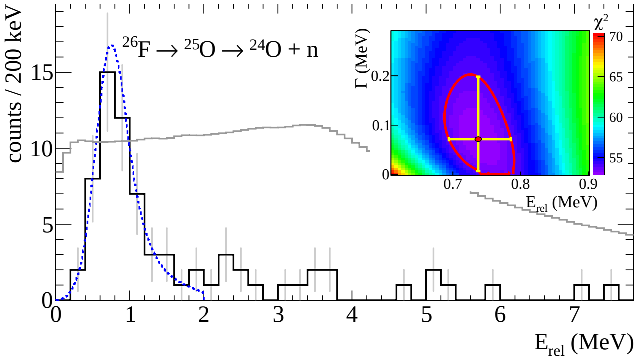

FIG. 1. (color online) Relative-energy spectrum of the ^{24}O+n system measured in a proton-knockout reaction from ^{26}F. The dotted curve shows a Breit-Wigner fit to the data. The grey histogram indicates the experimental response for a white spectrum. The inset displays χ^2 as a function of position and width, and indicates the minimum and the 1σ-contour.

From the measurements of the momenta of outgoing fragments and neutrons, the two- and three-body relative-energy spectra are reconstructed for one- and two-neutron events. Figure 1 shows the ^{24}O+n relative-

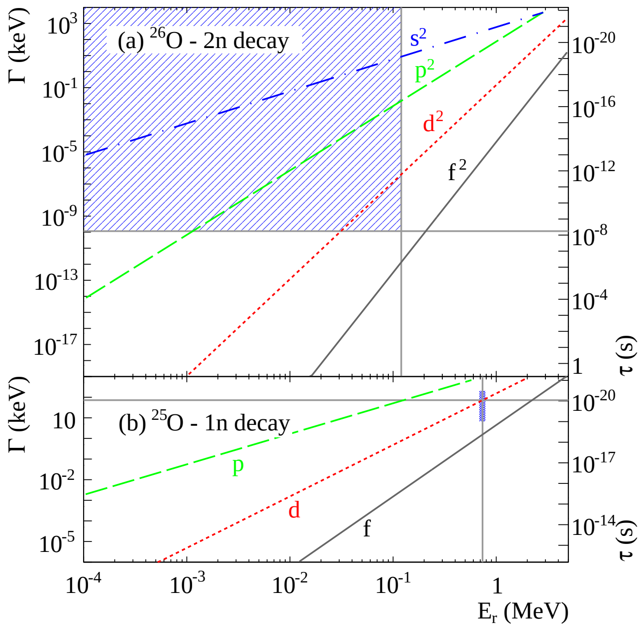

FIG. 2. (color online) Width and lifetime as a function of resonance energy for ^{26}O (upper panel) and ^{25}O (lower panel). The curves show theoretical expectations for different l-values of the neutron(s) from Ref. [10]. For ^{26}O, the upper limits for the resonance energy and lifetime are given by horizontal and vertical grey lines. The allowed region defined by these limits is represented by the shaded area. For ^{25}O, the present experimental results are given by the horizontal and vertical grey lines, with errors indicated by the shaded area.

energy spectrum after proton removal from ^{26}F. A prominent peak structure is visible at around 700 keV corresponding to the ground-state resonance of ^{25}O. The position and width of the resonance have been extracted by fitting a Breit-Wigner distribution with an energy-dependent width and a channel radius of 4 fm. For the χ^2 minimization procedure, Pearson's chi-square method [12], using errors of the parent distribution according to a Poisson probability distribution, has been used, as the usual method with errors estimated from the number of counts gives inaccurate results in case of low statistics. The 1σ-contour in the 2-dimensional parameter space is displayed in the inset of Fig. 1. The extracted position and width of 737^{+48}_{-43} keV and 72^{+126}_{-65} keV, respectively, are in good agreement with the previously reported values [4] within experimental errors, see Table I. The relatively large experimental error on the width is due to the instrumental energy resolution which dominates the apparent width. The measured width is also in agreement with the expectation of a d-state single-particle resonance with a spectroscopic factor of unity, as shown in the lower panel of Fig. 2 by the expected widths and lifetimes as a function of resonance position for different neutron angular momentum l (based on Ref. [10]).

The experimental relative-energy spectrum for ^{26}O is shown in Fig. 3. The upper panel displays events, where ^{24}O has been detected in coincidence with two neutrons. Two groups of events are observed: below 1 MeV and around 4 MeV. The shape of the experimental response, indicated by the grey histogram, is rather flat over the energy region shown, but exhibits a steep fall-off for small energies below 500 keV. For such small relative energies, the neutrons are not well separated in space and time when hitting the detector and can thus hardly be distinguished from 1n events. The effect can be seen quantitatively in the two-dimensional response matrices shown in Fig. 4. The energy reconstructed from the simulation is plotted versus the generated one in the lower panel, showing a band along the diagonal with a width reflecting the instrumental resolution. For low relative energies, the curve bends away from the diagonal and, in addition, the events are being reconstructed as 1n events with a large probability. This can be seen in the upper panel, which shows the reconstructed ^{24}O+n relative energy spectrum for the events falsely identified as 1n events. The simulation is based on measured real 1n events from deuteron breakup reactions. The 2n events are generated by overlaying the hit patterns from these measured 1n events and are then analyzed in the same way as the experimental data. The generated response matrices thus do not rely on a simulation of the neutron reactions in the detection process.

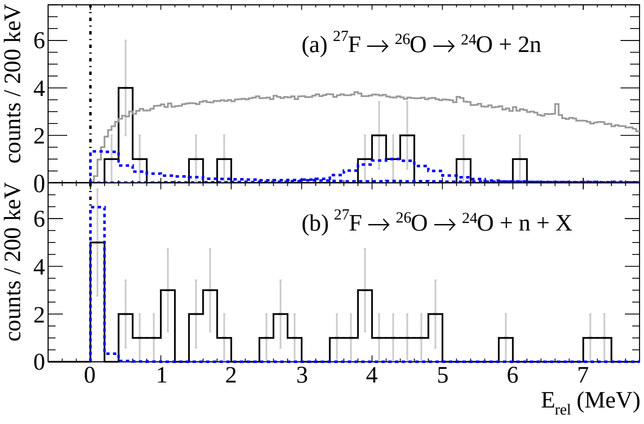

FIG. 3. (color online) One- and two-neutron channel measured in coincidence with ^{24}O after one-proton removal from ^{27}F. The histograms with error bars represent the measured ^{24}O+2n three-body relative-energy spectrum (top panel) and the ^{24}O+n+X relative-energy spectrum (bottom panel). The grey histogram indicates the experimental response for a white spectrum in the 2n channel. The dotted curves display the most probable fit to the data corresponding to two states in ^{26}O at 25^{+25}_{-25} keV and around 4 MeV (see text).

The effect discussed above is clearly visible in the ^{26}O data of Fig. 3. In the 1n channel (lower panel), the accumulation of events at very low energy in the first bin is striking. This is not present in the 1n events mea-

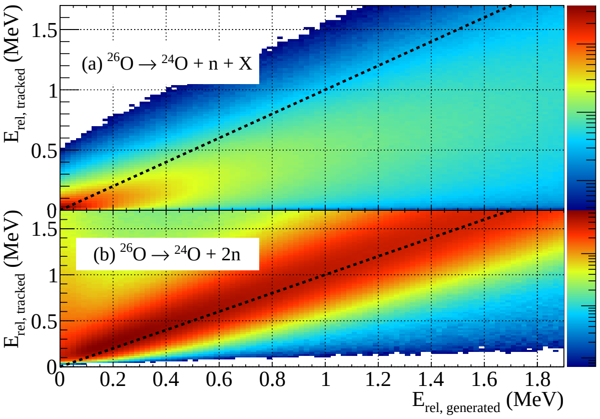

FIG. 4. (color online) Simulated instrumental response for detection of a $2n$ decay of ^{26}O with relative energy E_{rel}. The lower panel shows the extracted energy for two detected neutrons in coincidence with ^{24}O, while in the upper part, the ^{24}O+n relative energy spectrum is shown for events, where only one neutron has been detected due to inefficiency of the detector or the multi-neutron recognition algorithm.

TABLE I. Compilation of experimental and theoretical results obtained in this work compared to previously published results. All energies and lifetimes are given in keV and ns, respectively. Energies are measured from the gs energy of ^{24}O.

	E_r	Γ	τ	Ref.
^{25}O(gs)	737^{+48}_{-43}	72^{+126}_{-65}	$9.1^{+16}_{-8}\cdot 10^{-12}$	this work
	770^{+20}_{-10}	172^{+30}_{-30}	-	[4]
	733	NN+3N + residual 3N		this work
	1301/1303	USDA/B		[14]
	1002	-	-	[15]
^{26}O(gs)	$\leqslant 40/120$ [a]	$\geqslant 1.2\cdot 10^{-10}$ [b]	$\leqslant 5.7$ [c]	this work
	150^{+50}_{-150}	-	-	[8]
	18	NN+3N + residual 3N		this work
	501/356	USDA/B		[14]
	21	0.02	-	[15]
^{26}O(exc)	4225^{+227}_{-176}			this work

[a] 68%/95% c.l.
[b] from lifetime estimate, see text and Fig. 2
[c] 95% c.l.

sured in the proton knockout from ^{26}F, see Fig. 1. The events in the first bin of the ^{24}O+n spectrum are the characteristic fingerprint of a very low-lying state in ^{26}O. We have performed a simultaneous statistical analysis of $1n$ and $2n$ coincidences, starting with the hypothesis of a low-lying state in ^{26}O. The dotted histogram displays the most probable result yielding a position for the ^{26}O ground state of 25^{+25}_{-25} keV. Again, the χ^2 minimization using Poisson distributed errors of the test function has been used.

An alternative method [13], which is independent of the binning of the experimental data, is to use for each event the measured relative energy in conjunction with the inverse response matrix to calculate the probability distribution of the true energy (Bayesian approach with uniform prior). The resulting Bayesian interval goes from 0 to 40/120 keV for 68%/95% confidence limit (c.l.), including the $1n$ events at very low relative energy. From the energy measurement alone, we cannot exclude a very small value close to zero for position and width potentially leading to a rather long-lived ^{26}O ground state, which would constitute the first case of neutron radioactivity as speculated in Ref. [10]: As can be seen from Fig. 2, the lifetime for a d^2-state could reach seconds for a resonance position well below 1 keV. Such a long lifetime, however, can be excluded from the fragment measurement. The distance of the target to the middle of the dipole magnet measures 256 cm corresponding to a flight time of 11.8 ns. If ^{26}O decayed after that time, a fragment mass larger than 24 would be reconstructed by the tracking procedure. Also, no neutron coincidences should be observed in that case, since the fragment is bent by 7 degree after passing half of the dipole field. From the analysis of the energy spectra discussed above, the number of produced ^{26}O can be estimated. By triggering on proton knockout reactions using the Crystal Ball and vetoing on the neutron detector, the fragment-mass spectrum has been reconstructed for the ^{27}F$(p,2p)^{A}$O reaction. While we still observe events corresponding to ^{24}O, only one event appears above the ^{24}O cut at $A = 24.8$, which could potentially stem from a late decay in the dipole field. From this we obtain an upper limit for the lifetime of 5.7 ns with a 95% confidence limit. The upper limit for the position of the state and for its lifetime are shown in Fig. 2 leaving the shaded area as the allowed region. There is only a small overlap with the calculated values for a d^2-state, suggesting a more complex ^{26}O ground-state configuration.

It would therefore be very interesting to determine the lifetime experimentally more precisely in order to gain insights to the structure of ^{26}O. Such a measurement would be rather straightforward using a similar method as described here, but placing the target directly in front of the dipole. The decay curve of ^{26}O would translate into a fragment-mass spectrum distribution depending on the decay position. In addition, the neutrons will be detected not only at zero degree, but also in the bending direction, again directly reflecting the decay curve. With the intensities available, e.g., at the RIBF facility at RIKEN, a precise value could be obtained from such an experiment with the SAMURAI detector.

We compare the ground-state energies of ^{25,26}O to theoretical shell-model calculations based on chiral effective field theory interactions combined with renormalization-group methods to evolve nuclear forces to lower resolution [16]. Our results are based on chiral NN and 3N forces, where the single-particle energies and two-body

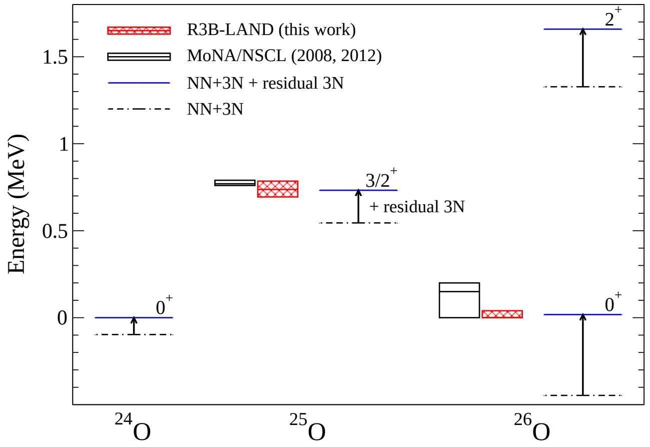

FIG. 5. (color online) Comparison of the experimental ^{25}O and ^{26}O energies with theoretical shell-model calculations based on chiral NN and 3N forces (NN+3N) and including residual 3N forces. The impact of residual 3N forces is highlighted by the arrows.

interactions of valence neutrons on top of a ^{16}O core are calculated following Refs. [17, 18], without adjustments. Here, we focus on the relative contribution from residual three-valence-neutron forces, which become more important with neutron number along isotopic chains [19]. Figure 5 shows the predicted ground-state energies. The relative contribution from residual 3N forces, which we included perturbatively, increases from 0.1 to 0.4 MeV for $^{24-26}$O. Because the ground states of ^{25,26}O are very narrow, thus quasi-bound, they can be treated fairly well in a bound-state approximation. The remarkable agreement with experiment should, however, be taken with care, as the continuum needs to be included. The expected contribution is 200 keV to both ^{25,26}O [20], so relative energy differences will be smaller. We have also explored uncertainties in the calculation of the single-particle energies and valence interactions, which would increase the ground-state energy relative to ^{24}O for ^{25,26}O by $0.2-0.3$ MeV. In Table I, we also compare with the phenomenological USDA/B interactions [14], which predict too high energies for ^{25,26}O. Better agreement is found in Table I for the continuum shell model [15], see also the promising continuum developments of Refs. [20, 21].

The theoretical calculations based on chiral NN and 3N forces predict a first excited 2^+ state in ^{26}O at 1.6 MeV relative to the ^{26}O ground state. It is found at 1.9/2.1 MeV for USDA/B interactions and at 1.8 MeV for Ref. [15]. Experimentally, the events at 4 MeV in the three-body energy spectrum (top panel of Fig. 3) provide evidence for an excited state in ^{26}O, with most probable energy 4225^{+227}_{-176} keV. A likely candidate would be a proton-hole state populated after knockout from the ^{27}F $0p_{1/2}$ shell (rather than from the $0d_{5/2}$ valence orbital). To investigate proton (and neutron) cross-shell excitations, we have carried out $(0+1)\hbar\omega$ calculations in the *spsdpf* space using the WBP interaction [22], for which the first and second 2^+ energies are at 2.3 and 5.4 MeV, repectively. The first state with a proton excitation component from $0p_{1/2}$ to $0d_{5/2}$ is a 3^- state at higher energy of 5.4 MeV, whose proton contributon is also mixed with neutron excitations and considerably weaker than for the corresponding 3^- state at 5.0 MeV in ^{18,20}O. Note that ^{26}O is bound by 1.0 MeV for the WBP interaction, so that 1 MeV uncertainties are possible. The lowest negative parity states predicted by the WBP interaction are a quartet of $3^-, 2^-, 1^-, 0^-$ neutron excitations from $0d_{3/2}$ to $1p_{3/2}$ at 3.7, 4.1, 4.5, 4.9 MeV (with centroid at 4.1 MeV). Because of strong proton-neutron interactions, the proton-knockout reaction mechanism could also be more involved, generating admixed neutron excitations.

In this first R3B-LAND experiment, we have investigated the ground-state energy, width, and lifetime of the unbound oxygen isotopes ^{25}O and ^{26}O. Our results are in very good agreement with theoretical shell-model calculations based on chiral NN and 3N forces, where the ground-state energy of these extremely neutron-rich isotopes becomes increasingly sensitive to 3N forces among the valence neutrons. The ^{26}O ground state is unbound by less than 120 keV, and our measurement for the lifetime $\leqslant$5.7 ns (both at 95% c.l.) excludes ^{26}O being a first candidate for neutron radioactivity. We have proposed an experiment with existing detectors to determine the ^{26}O lifetime accurately, which would yield important information on the ground-state nature of ^{26}O. We also obtained first evidence for an excited state of ^{26}O located at around 4 MeV. Different possibilities for the nature of this state exist, making it an exciting case for future calculations and experiments with higher resolution.

We thank B. A. Brown for helpful discussions on the WBP interaction. This work was supported by the Helmholtz International Center for FAIR within the framework of the LOEWE program launched by the state of Hesse, by the Helmholtz Alliance Program of the Helmholtz Association, contract HA216/EMMI "Extremes of Density and Temperature: Cosmic Matter in the Laboratory", by the GSI-TU Darmstadt Cooperation agreement, and by the BMBF under Contracts No. 06DA70471, 06DA9040I, 06MT238, the DFG cluster of excellence Origin and Structure of the Universe, the US DOE Grants DE-FC02-07ER41457, DE-FG02-96ER40963, and the Portuguese FCT, project PTDC/FIS/103902/2008.

---

[*] E-mail: t.aumann@gsi.de

[†] present address: TRIUMF, 4004 Wesbrook Mall, Vancouver, BC V6T 2A3, Canada

[1] T. Baumann, A. Spyrou, and M. Thoennessen, Rep. Prog. Phys. **75**, 036301 (2012).

[2] H. Sakurai *et al.*, Phys. Lett. B **448**, 180 (1999).
[3] T. Otsuka, T. Suzuki, J. D. Holt, A. Schwenk, and Y. Akaishi, Phys. Rev. Lett. **105**, 032501 (2010).
[4] C. R. Hoffman *et al.*, Phys. Rev. Lett. **100**, 152502 (2008).
[5] R. Kanungo *et al.*, Phys. Rev. Lett. **102**, 152501 (2009).
[6] R. V. F. Janssens, Nature **459**, 1069 (2009).
[7] T. Otsuka, T. Suzuki, R. Fujimoto, H. Grawe, and Y. Akaishi, Phys. Rev. Lett. **95**, 232502 (2005).
[8] E. Lunderberg *et al.*, Phys. Rev. Lett. **108**, 142503 (2012).
[9] G. Christian *et al.*, Phys. Rev. Lett. **108**, 032501 (2012).
[10] L. V. Grigorenko, I. G. Mukha, C. Scheidenberger, and M. V. Zhukov, Phys. Rev. C **84**, 021303 (2011).
[11] R. Palit *et al.*, Phys. Rev. C **68**, 034318 (2003).
[12] S. Baker and R. Cousins, NIMPR **221**, 437 (1984).
[13] P. Bevington and D. Robinson, *Data Reduction and Error Analysis for the Physical Sciences*, 2nd ed. (McGraw-Hill, New York, 1992).
[14] B. A. Brown and W. A. Richter, Phys. Rev. C **74**, 034315 (2006).
[15] A. Volya and V. Zelevinsky, Phys. Rev. C **74**, 064314 (2006).
[16] S. K. Bogner, R. J. Furnstahl, and A. Schwenk, Prog. Part. Nucl. Phys. **65**, 94 (2010).
[17] J. D. Holt, J. Menéndez, and A. Schwenk, (2011), arXiv:1108.2680.
[18] A. T. Gallant *et al.*, Phys. Rev. Lett. **109**, 032506 (2012).
[19] B. Friman and A. Schwenk, in *From Nuclei to Stars: Festschrift in Honor of Gerald E. Brown*, edited by S. Lee (World Scientific, 2011) p. 141, arXiv:1101.4858.
[20] G. Hagen, M. Hjorth-Jensen, G. R. Jansen, R. Machleidt, and T. Papenbrock, Phys. Rev. Lett. **109**, 032502 (2012).
[21] K. Tsukiyama, M. Hjorth-Jensen, and G. Hagen, Phys. Rev. C **80**, 051301 (2009).
[22] E. K. Warburton, J. A. Becker, and B. A. Brown, Phys. Rev. C **41**, 1147 (1990).